Available online at www.sciencedirect.com
ScienceDirect
Nuclear Physics A 857 (2011) 1–8
NUCLEAR PHYSICS A
www.elsevier.com/locate/nuclphysa

α-Spectroscopic factor of $^{16}O_{gs}$ from the $^{12}C(^{16}O,^{12}C)^{16}O$ reaction

M.C. Morais, R. Lichtenthäler *

Instituto de Fisica, Universidade de São Paulo, C.P. 66318, 05389-970 São Paulo, Brazil

Received 24 December 2010; received in revised form 3 March 2011; accepted 9 March 2011

Available online 15 March 2011

Abstract

Elastic scattering angular distributions of $^{16}O + ^{12}C$ in the center of mass energy range from 8.55 MeV to 56.57 MeV have been analyzed considering the effect of the exchange of an alpha particle between projectile and target leading to the same nuclei of the entrance channel (elastic-transfer). An alpha particle spectroscopic factor for the ground state of the ^{16}O was determined.

Keywords: Low energy elastic scattering; Alpha-transfer reactions; Optical model; DWBA; Spectroscopic factor; Alpha cluster

1. Introduction

Alpha clustering in nuclei has been a subject of intense investigations since the 1950's until nowadays [1–3]. Light nuclei composed of an integer number of alpha particles such as ^{8}Be, ^{12}C, ^{16}O and others (α-nuclei) are known to present excited levels which are well described in terms of alpha cluster models. The well-known Hoyle state in ^{12}C [4] has a triple-alpha structure at 7.65 MeV excitation energy, just above the 7.27 MeV $^{8}Be + \alpha$ threshold, which is responsible for the carbon synthesis in the universe. Several excited states of the ^{16}O are also known to present considerably large α-spectroscopic factors and can be well described in terms of an $\alpha + ^{12}C$ cluster model [5].

Another indication of α-clustering is the large α-transfer cross section observed in heavier α-systems such as $^{16}O + ^{24}Mg$, $^{12}C + ^{24}Mg$ and $^{16}O + ^{28}Si$. The Anomalous Large Angle Scat-

* Corresponding author.
E-mail address: rubens@if.usp.br (R. Lichtenthäler).

0375-9474/$ – see front matter
doi:10.1016/j.nuclphysa.2011.03.005

tering (ALAS) observed in those systems, is characterized by an enhancement of the backward angles differential cross section of the elastic, inelastic scattering and α-transfer reactions and was extensively studied during the 1970 and 1980 [6]. The excitation functions of the elastic scattering and reactions also present resonant-like structures which have been partially explained in terms of the coupling to α-transfer channels [7,8].

Although, for the heavier systems cited above the role of the elastic-transfer process is not totally established, in the case of lighter systems of adjacent masses its importance has been recognized since earlier [9]. The alpha particle transfer from the ^{16}O to the ^{12}C leads to the same nuclei of the entrance channel and might have an important contribution to the $^{16}\mathrm{O} + {}^{12}\mathrm{C}$ elastic scattering. The enhancement observed at backward angles in the $^{16}\mathrm{O} + {}^{12}\mathrm{C}$ elastic angular distribution is probably due to the contribution of the elastic-transfer process $^{12}\mathrm{C}(^{16}\mathrm{O},^{12}\mathrm{C})^{16}\mathrm{O}$, since the backward angles of the elastic correspond to the forward angles of the transfer process.

A large amount of complete angular distributions of $^{16}\mathrm{O} + {}^{12}\mathrm{C}$ scattering is available in the literature and transfer codes [10] exist which include finite-range and recoil effects exactly allowing a quantitative investigation of the effect of the elastic-transfer process.

In this paper we present a systematic analysis of elastic angular distributions of $^{16}\mathrm{O} + {}^{12}\mathrm{C}$ at several energies ranging from below up to about 6 times the Coulomb barrier. An Optical Model analysis was performed using a double folding potential [11] for the real part and a volume Woods–Saxon for the imaginary potential whose parameters were adjusted to reproduce the angular distributions at the forward angles. The effect of the elastic-transfer process was taken into account in first order by adding the DWBA (Distorted Waves Born Approximation) transfer amplitude to the elastic one. The $\alpha + {}^{12}\mathrm{C}$ spectroscopic factor normalizes the transfer amplitude and was adjusted to reproduce the backward angles cross section.

2. Analysis of the elastic scattering angular distributions

Both process, elastic scattering and elastic-transfer, are experimentally indistinguishable and their amplitudes must be added taking into account that $\theta_{c.m.}^{elastic} = \pi - \theta_{c.m.}^{transfer}$. The total elastic scattering differential cross section can thus be written as:

$$\frac{d\sigma}{d\Omega}(\theta) = \left| f^{(0)}(\theta) + f_{transfer}(\pi - \theta) \right|^2 \tag{1}$$

The zero order elastic amplitude $f^{(0)}(\theta)$ was calculated in the Optical Model ($U(r) = V(r) + iW(r)$) using the double folding potential [11] for the real part $V(r) = N_r \times V_{fold}(r)$ and a usual volume Woods–Saxon shape

$$W(r) = \frac{W_0}{1 + \exp(\frac{r - R_i}{a_i})} \tag{2}$$

for the imaginary part. The normalization N_r of the real potential and W_0, R_i, a_i were adjusted to reproduce the angular distributions at forward angles where the elastic amplitude dominates.

The transfer amplitude has been calculated in DWBA using the FRESCO [10] program and added to the elastic one as stated in Eq. (1). For the elastic transfer process $^{12}\mathrm{C}(^{16}\mathrm{O},^{12}\mathrm{C})^{16}\mathrm{O}$ the DWBA amplitude simplifies to:

$$T^{DWBA} = \int d\mathbf{r} \chi^{(-)*}(\mathbf{r}) \left\langle S^{1/2} \varphi(\xi) \left| V_{\alpha C} + U_{CC} - U(\mathbf{r}) \right| S^{1/2} \varphi(\xi) \right\rangle \chi(\mathbf{r}) \tag{3}$$

with $f_{transfer}(\theta) = \frac{2\pi}{\hbar}\sqrt{\mu_\alpha \mu_\beta}\frac{k_\alpha}{k_\beta}|T^{DWBA}|^2$. $\chi(\mathbf{r})$ is the distorted wave function and has been obtained from the elastic scattering analysis. U_{CC} is the core–core potential and $V_{\alpha C}$ is the α-carbon bound state potential. As core–core potential U_{CC} we used the São Paulo Optical Potential [11] with the usual normalization $N_i = 0.78$ of the imaginary part. The bound state wave function $\varphi_{\alpha+^{12}C}(\xi)$ depends of the internal coordinates and was generated by solving the Schrödinger equation in a real Woods–Saxon well $V_{\alpha C}$ of radius $R = 1.06 \times (12^{1/3} + 4^{1/3}) = 4.11$ fm and diffuseness $a = 0.35$ fm (WS2). The parameters have been obtained from elastic scattering data of $\alpha+^{12}$C at low energy [12]. Here a diffuseness lower than the standard usual value $a = 0.65$ fm is used in agreement with results of the analysis of alpha scattering [13] on heavier targets. The depth of the potential was adjusted to reproduce the binding energy $E = 7.16$ MeV of the ^{16}O ground state. The number of nodes of the bound state wave function was determined by the Wildermuth condition [14]: $2N + L = \sum_{i=1}^{4}(2n_i + l_i)$, where N is the number of nodes, L is the angular momentum of the alpha cluster ($N = 3$ including the origin and $L = 0$ for the $^{16}O_{gs}$) and n_i and l_i are the quantum numbers of the Fermi levels ($0p_{1/2}$) occupied by the nucleons of the alpha cluster in the ^{16}O. The spectroscopic amplitude $S^{1/2}_{\langle^{16}O_{gs}|^{12}C\rangle}$ normalizes the bound states wave function and was adjusted to reproduce the intermediate and backward angles cross section.

3. Results and discussion

Experimental data of twenty angular distributions [15–17] have been analyzed. In Figs. 1 and 2, we show the fits and in Table 1 the corresponding optical model parameters and spectroscopic factors obtained.

Two calculations are presented, the dashed curves are the cross-sections obtained using the elastic amplitude $f^{(0)}(\theta)$ only, without considering the elastic-transfer and the solid curve is the complete calculation, including the effect of the transfer. We observe that, at the lower energies, the elastic amplitude dominates at forward angles and competes with the transfer amplitude in the intermediate and backward angles region. As the energy increases the elastic amplitude drops down and becomes less and less important at backward angles while the transfer dominates. For instance, at $E_{c.m.} = 21.86$ MeV the elastic contribution is about 2 orders of magnitude lower than the transfer at large angles near 180 deg. We see that above $E_{c.m.} \approx 20$ MeV and for backward angles ($\theta > 140$ deg), the cross section is dominated by the elastic transfer process and can thus be used to determine the $\alpha + {}^{12}\mathrm{C} = {}^{16}\mathrm{O}_{gs}$ spectroscopic factor.

3.1. Spectroscopic factors and Asymptotic Normalization Coefficients (ANC)

The resulting spectroscopic factors are presented in Table 1 and in Fig. 3. We see in Fig. 3 that the spectroscopic factors show fluctuations with the energy which are probably due to the well-known resonant-like behavior observed in the $^{16}\mathrm{O} + {}^{12}\mathrm{C}$ excitation functions [18]. The average of $N = 20$ values listed in Table 1 gives $\langle S_\alpha \rangle = 1.58(10)$ where we quote the estimated error of the mean as $\sigma_{sd}/\sqrt{(N)}$ where σ_{sd} is the standard deviation. If the outlying values at $E = 13.01, 17.28, 19.40, 25.50$ MeV are disregarded, the standard deviation is considerably reduced and the average value is decreased by about 9% to $S_\alpha = 1.45(3)$. The best fit at $E = 23.14$ MeV gives $S_\alpha = 1.59$.

A critical point in the DWBA analysis is the choice of the binding potential $\alpha+^{12}$C which defines the transfer form factor of the DWBA integral. The spectroscopic factors are in gen-

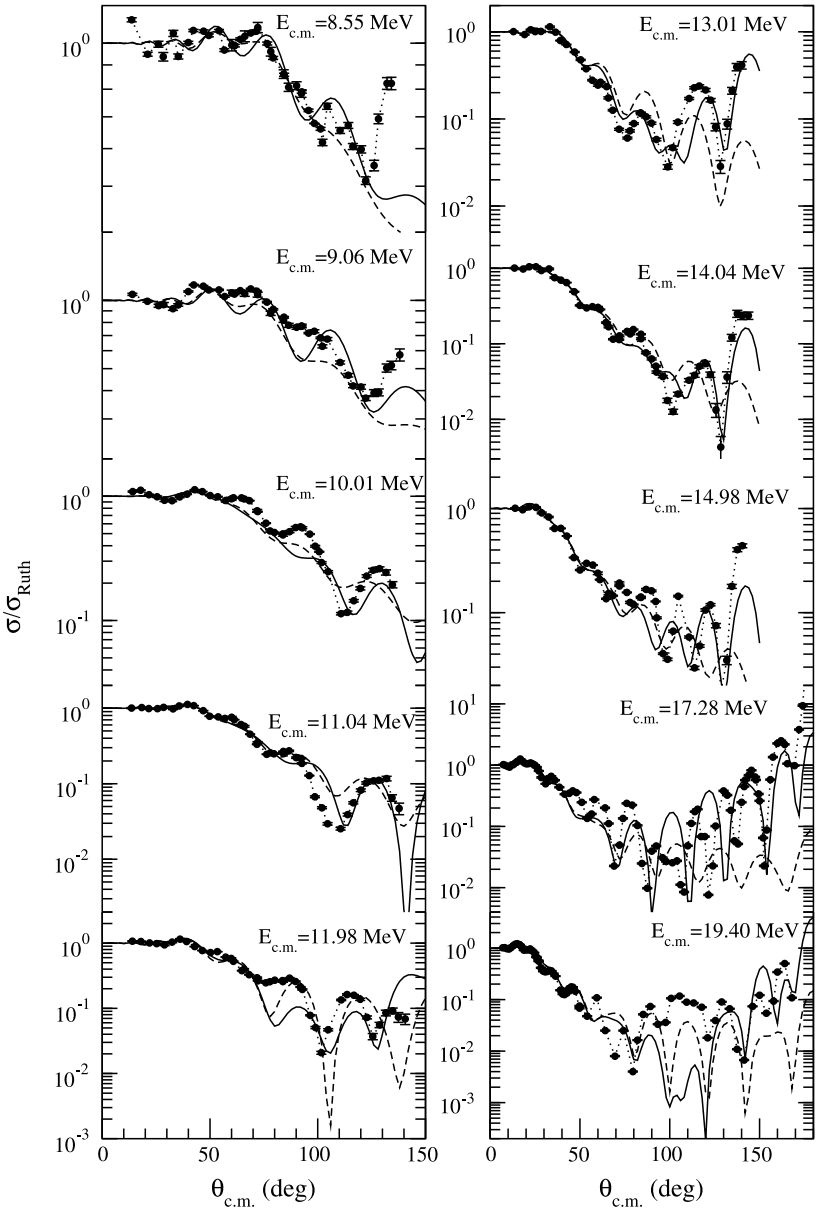

Fig. 1. $^{16}O + ^{12}C$ angular distributions (squares). The solid line is the result of the calculation considering the effect of the elastic-transfer. Dashed line is optical model only. The dotted line is a guide to the eyes.

eral dependent of the binding potential parameters. To investigate this dependence, in Fig. 4 we compare the results with three different potentials, the WS2 used in the present analysis, a potential determined from a folding procedure [20] and a standard potential (WS1) with $R = 1.25 \times (12^{1/3} + 4^{1/3}) = 4.85$ fm and diffuseness $a = 0.65$ fm. In both cases the depths of the potentials were adjusted to reproduce the binding energy and the number of nodes of the

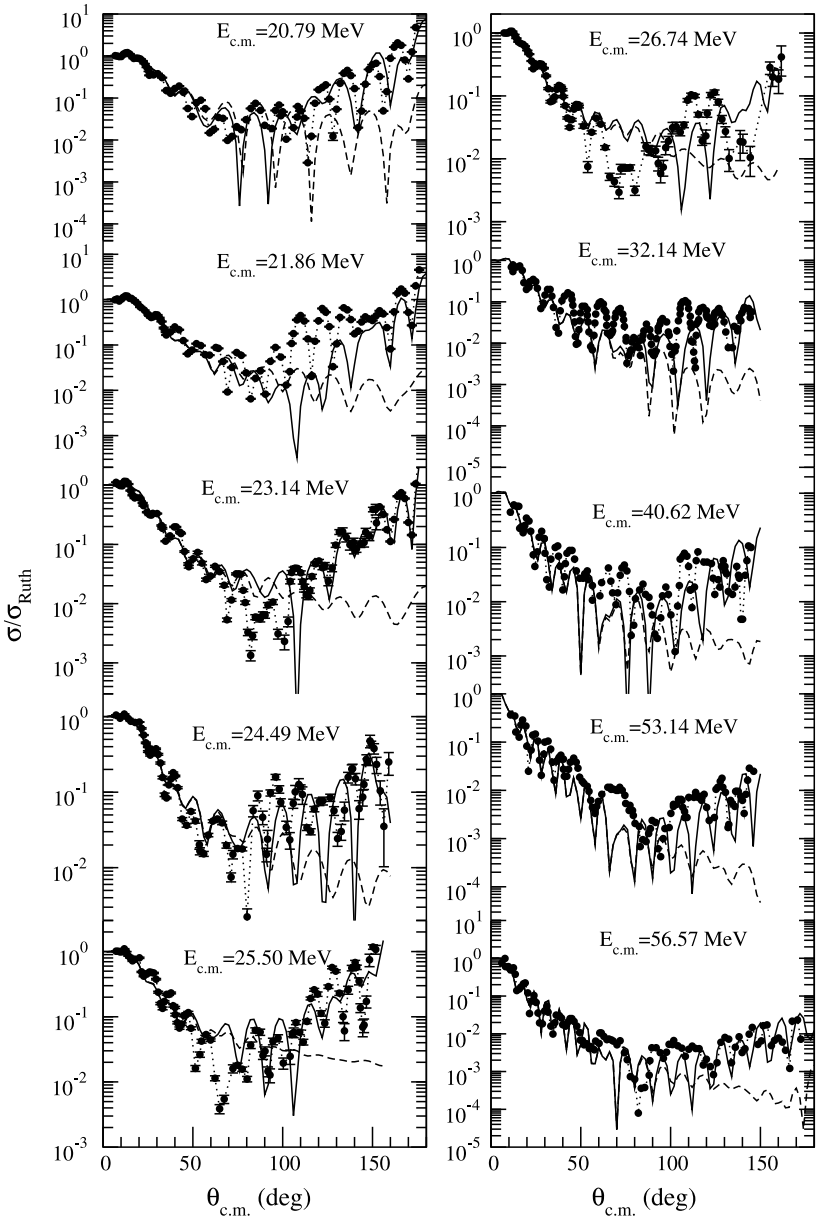

Fig. 2. $^{16}O + ^{12}C$ angular distributions (squares). The solid line is the result of the calculation considering the effect of the elastic-transfer. Dashed line is optical model only. The dotted line is a guide to the eyes.

$\alpha+^{12}C$ wave function. The obtained values of the spectroscopic factors are $S_{WS1} = 1.08$ and $S_{folding} = 1.96$. A similar dependence of the spectroscopic factors with the geometry of the binding potential has been observed in other works [9,21]. However, as the shape of the experimental angular distributions at backward angles are much better reproduced by the potential WS2 we take this as our main result.

Table 1
Parameters of the optical potential and spectroscopic factors. V is the depth of the folding potential at $r = 0$ fm.

$E_{c.m.}$ (MeV)	W_0 (MeV)	r_i (fm)	a_i (fm)	N_r	V (10^2 MeV)	Spectroscopic factors
8.55	3.32	1.48	0.45	0.83	2.75	1.23
9.06	3.38	1.48	0.45	0.83	2.75	1.51
10.01	3.29	1.55	0.40	1.11	3.68	1.49
11.04	3.51	1.50	0.45	1.10	3.65	1.28
11.98	2.87	1.40	0.45	0.87	3.23	1.28
13.01	4.25	1.50	0.45	0.85	2.82	2.10
14.04	4.83	1.51	0.45	0.84	2.77	1.39
14.98	5.30	1.50	0.35	0.84	2.78	1.37
17.28	7.30	1.37	0.30	0.87	2.87	2.13
19.40	6.05	1.38	0.30	0.81	2.67	1.01
20.79	6.00	1.39	0.30	0.82	2.70	1.61
21.86	8.20	1.37	0.30	0.80	2.63	1.51
23.14	10.51	1.35	0.30	0.88	2.92	1.59
24.49	8.79	1.38	0.30	0.82	2.69	1.56
25.50	11.97	1.39	0.30	0.86	3.28	3.13
26.74	11.00	1.37	0.30	0.85	2.95	1.59
32.14	9.65	1.34	0.40	0.80	2.61	1.49
40.62	9.65	1.35	0.40	0.75	2.44	1.51
53.14	12.70	1.34	0.40	0.78	2.50	1.46
56.57	12.31	1.33	0.40	0.75	2.39	1.25

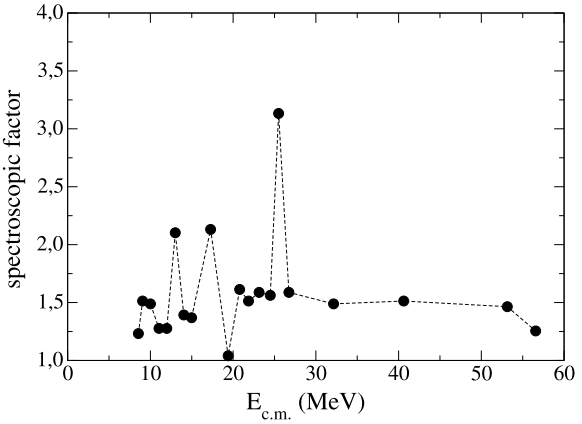

Fig. 3. Spectroscopic factors obtained as a function of the energy of the angular distributions. The dashed line is a guide to the eyes.

In Table 2 we compare our results to others from the literature. Several works have been performed in the past to obtain the ^{16}O spectroscopic factor using the ^{12}C(^{6}Li, d)^{16}O and ^{12}C(^{7}Li, t)^{16}O reactions [22–25]. More recently the ^{16}O breakup [26] has been analyzed by Continuum Discretized Coupled Channels calculations CDCC and the ground state spectroscopic factor and ANC have been obtained. We see that our spectroscopic factor is in reasonable agreement with other works [9,19] that used the same reaction but in disagreement with the works that use the ^{12}C(^{6}Li, d) and ^{12}C(^{7}Li, t) reactions.

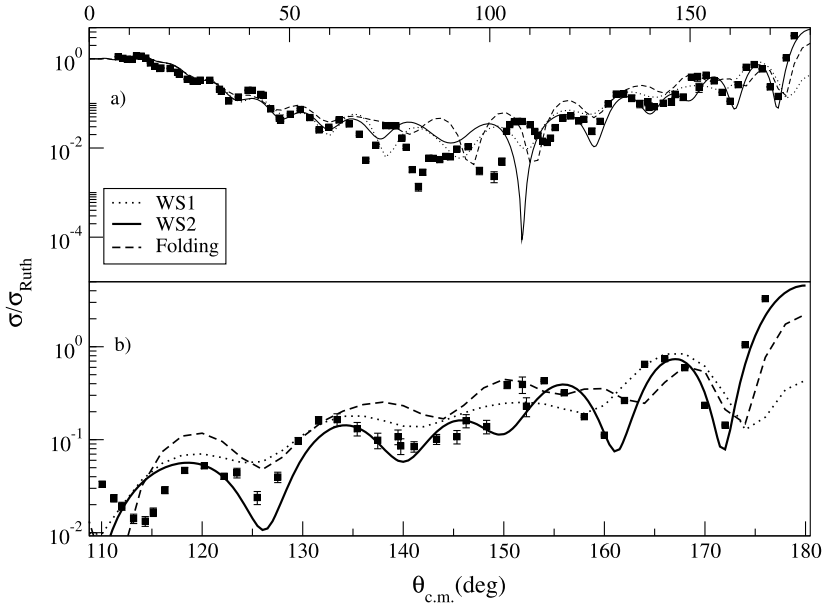

Fig. 4. $^{16}O + {}^{12}C$ angular distribution at $E_{c.m.} = 23.14$ MeV (squares). a) The solid line is the result of the calculation with the effect of the elastic-transfer using binding potential WS2. The dotted line uses WS1 and the dashed line the folding potential (see text). b) is a zoom in the backward angles region.

Table 2
Alpha spectroscopic factors for $^{16}O_{gs}$.

Work	Reaction	S_α
This work	$^{12}C(^{16}O,^{12}C)^{16}O$	1.45–1.58
Refs. [22,23]	$^{12}C(^{6}Li, d)^{16}O$	7.6–10
Ref. [24]	$^{12}C(^{7}Li, t)^{16}O$	0.38
Ref. [25]	$^{12}C(^{6}Li, d)^{16}O$	0.34
Ref. [26]	$^{16}O \rightarrow \alpha + {}^{12}C$	5.41
Refs. [9,19]	$^{12}C(^{16}O,^{12}C)^{16}O$	1.0–2.0

The ANC coefficient is given by $C^2 = S_\alpha b^2$ where $b = \varphi(r)/W(r)$ is the single-particle ANC calculated as the ratio between the bound state wave function and the Whittaker function in the asymptotic region ($r \rightarrow \infty$). We obtained $C^2 = 1.51 \times 10^6$ fm^{-1} for the potential WS2 and $C^2 = 1.15 \times 10^7$ fm^{-1} and $C^2 = 5.6 \times 10^5$ fm^{-1} respectively for the WS1 and folding potentials. $C^2 = 194.786$ fm^{-1} was obtained in Ref. [26]. It is expected that, for peripheral reactions involving weakly bound nuclei, the ANC would be less sensitive to the bound state potential parameters however this is obviously not the case here, probably due to the fact that the α-transfer $^{12}C(^{16}O,^{12}C)^{16}O_{gs}$ cannot be considered as a peripheral reaction.

4. Conclusions

A systematic analysis of a total of twenty elastic angular distributions of $^{16}O + {}^{12}C$ has been performed considering the effect of the elastic-transfer of an alpha particle. We found that the elastic-transfer is probably the process responsible for the backward rise of the differential cross

section and becomes dominant as the bombarding energy increases. An average value of the $S_{\langle^{12}\mathrm{C}|^{16}\mathrm{O}_{gs}\rangle}$ spectroscopic factor has been obtained. The results presented here may have some importance in further indirect determinations of the $^{12}\mathrm{C} + \alpha$ rate.

Acknowledgements

This work has been supported by Fundação de Amparo à Pesquisa do Estado de São Paulo (FAPESP), proc. No. 2008/09341-7, and by the Conselho Nacional de Desenvolvimento Científico e Tecnológico (CNPq) and the CAPES (Comissão de Aperfeiçoamento do Ensino Superior).

References

[1] W. von Oertzen, M. Freer, Y. Kanada-En'yo, Phys. Rep. 432 (2006) 43.
[2] K. Ikeda, et al., Prog. Theor. Phys. Suppl. 68 (1980) 1.
[3] Y. Fujiwara, et al., Prog. Theor. Phys. Suppl. 68 (1980) 29.
[4] M. Chernykh, H. Feldmeier, T. Neff, P. von Neumann-Cosel, A. Richter, Phys. Rev. Lett. 98 (2007) 032501.
[5] Y. Suzuki, Prog. Theor. Phys. 55 (1976) 1751.
[6] P. Braun-Munzinger, J. Barrette, Phys. Rep. 87 (1982) 209.
[7] R. Lichtenthäler Filho, A. Lépine-Szily, A.C.C. Villari, O. Portezan Filho, Phys. Rev. C 39 (1989) 884.
[8] A. Lépine-Szily, R. Lichtenthäler Filho, M.M. Obuti, J. Martins de Oliveira Jr., O. Portezan Filho, W. Sciani, A.C.C. Villari, Phys. Rev. C 40 (1989) 681.
[9] W. von Oertzen, H.G. Bohlen, Phys. Rep. 19 (1975) 1.
[10] I.J. Thompson, Comput. Phys. Rep. 7 (1988) 167.
[11] L.C. Chamon, B.V. Carlson, L.R. Gasques, D. Pereira, C. De Conti, M.A.G. Alvarez, M.S. Hussein, M.A. Cândido Ribeiro, E.S. Rossi, C.P. Silva, Phys. Rev. C 66 (2002) 014610.
[12] C.M. Perey, F.G. Perey, At. Data Nucl. Data Tables 17 (1976) 1.
[13] P. Mohr, et al., Phys. Rev. C 82 (2010) 044606.
[14] G.R. Satchler, Direct Nuclear Reactions, Oxford University Press, New York, 1983, p. 721.
[15] A.C.C. Villari, A. Lépine-Szily, R. Lichtenthäler Filho, O. Portezan Filho, M.M. Obuti, J.M. Oliveira Jr., N. Added, Nucl. Phys. A 501 (1989) 605.
[16] M.P. Nicoli, F. Haas, R.M. Freeman, S. Szilner, Z. Basrak, A. Morsad, G.R. Satchler, M.E. Brandan, Phys. Rev. C 61 (2000) 034609.
[17] A.A. Ogloblin, Yu.A. Glukhov, W.H. Trzaska, A.S. Dem'yanova, S.A. Goncharov, R. Julin, S.V. Klenibkov, M. Mutterer, M.V. Rozhkov, V.P. Rudakov, G.P. Tiorin, Dao T. Khoa, G.R. Satchler, Phys. Rev. C 62 (2000) 044601.
[18] R.E. Malmin, R.H. Siemssen, D.A. Sink, P.P. Singh, Phys. Rev. Lett. 28 (1972) 1590.
[19] S. Szilner, W. von Oertzen, Z. Basrak, M. Milin, F. Haas, Eur. Phys. J. A 13 (2002) 273.
[20] B. Buck, C.B. Dover, J.P. Vary, Phys. Rev. C 11 (1975) 1803.
[21] R.M. DeVries, Nucl. Phys. A 212 (1973) 207.
[22] F.D. Becchetti, J. Jänecke, C.E. Thorn, Nucl. Phys. A 305 (1978) 313.
[23] F.D. Becchetti, D. Overway, J. Jänecke, W.W. Jacobs, Nucl. Phys. A 344 (1980) 336.
[24] F.D. Becchetti, E.R. Flynn, D.L. Hanson, J.W. Sunier, Nucl. Phys. A 305 (1978) 293.
[25] A. Belhout, et al., Nucl. Phys. A 793 (2007) 178.
[26] S. Adhikari, C. Basu, Phys. Lett. B 682 (2009) 216.